

**Table VI—Values of Kinetic Parameters for 4-Aminoantipyrine-Induced Overtum of Goldfish**

Parameter	From Eq. 8 and Dose-Response Data	Literature Values	Reference
$k_1$	$6.54 \times 10^{-3} \text{ min.}^{-1}$	$2.3 \times 10^{-3} \text{ min.}^{-1}$	11
$k_2$	$6.54 \times 10^{-3} \text{ min.}^{-1}$	$3.3 \times 10^{-3} \text{ min.}^{-1}$	11
$C_p^*$	6.67 mg. %	6.8 mg. %	9

The proposed model for the action of homologous narcotic drugs on goldfish was tested using *n*-alkyl *p*-aminobenzoates. The experimental data were interpretable by the derived equations. Apparent discrepancies between the model and high concentration data were accounted for by recognizing that there is a finite lag time for turnover.

Literature data for 4-aminoantipyrine-induced narcosis of goldfish were also interpretable by the model.

#### REFERENCES

- (1) G. Levy and S. P. Gucinski, *J. Pharmacol. Exp. Ther.*, **146**, 80(1964).
- (2) G. Levy and K. E. Miller, *J. Pharm. Sci.*, **53**, 1301(1964).
- (3) *Ibid.*, **54**, 1319(1965).

- (4) N. A. Hall and W. L. Haydon, *J. Pharm. Sci.*, **56**, 304(1967).
- (5) M. Gibaldi and C. H. Nightingale, *ibid.*, **57**, 226(1968).
- (6) *Ibid.*, **57**, 1354(1968).
- (7) A. R. DiSanto and J. G. Wagner, *J. Pharm. Sci.*, **58**, 1077(1969).
- (8) C. H. Nightingale and M. Gibaldi, *ibid.*, **60**, 1360(1971).
- (9) C. H. Nightingale, *ibid.*, **60**, 1762(1971).
- (10) G. Levy and J. A. Anello, *ibid.*, **57**, 101(1968).
- (11) J. A. Anello and G. Levy, *ibid.*, **58**, 721(1969).
- (12) E. S. Manley and J. Belote, *ibid.*, **61**, 1401(1972).
- (13) M. Polonovski and A. Lindenberg, *C. R. Soc. Biol.*, **128**, 800(1938).
- (14) L. O. Ellisor and C. H. Richardson, *J. Cell. Comp. Physiol.*, **11**, 377(1938).
- (15) G. L. Flynn and S. H. Yalkowsky, *J. Pharm. Sci.*, **61**, 838(1972).
- (16) S. H. Yalkowsky, G. L. Flynn, and T. G. Slunick, *ibid.*, **61**, 853(1972).
- (17) J. Fergusson, *Proc. Roy. Soc.*, **127B**, 387(1939).

#### ACKNOWLEDGMENTS AND ADDRESSES

Received March 30, 1973, from the *Pharmacy Research Unit, The Upjohn Company, Kalamazoo, MI 49001*

Accepted for publication August 2, 1973.

▲ To whom inquiries should be directed.

## Correlation of Viscoelastic Functions for Pharmaceutical Semisolids: Comparison of Creep and Oscillatory Tests for Oil-in-Water Creams Stabilized by Mixed Emulsifiers

G. M. ECCLESTON<sup>▲</sup>, B. W. BARRY, and S. S. DAVIS\*

**Abstract** □ Liquid paraffin-in-water emulsions stabilized by mixed emulsifiers of a surfactant (cetrimide or cetomacrogol) and a long-chain alcohol were used as model systems to represent pharmaceutical semisolids. They were examined in their linear viscoelastic regions using creep and oscillatory (Weissenberg rheogoniometer) techniques. Storage and loss compliances ( $J'$  and  $J''$ ) over the frequency range  $2.5 \times 10^{-3}$  to  $1.5 \times 10^{-1}$  Hz. were calculated from creep data using numerical formulas. The transformed compliances were used to derive the other oscillatory functions, the storage and loss moduli ( $G'$  and  $G''$ ), the storage and loss viscosities ( $\eta'$  and  $\eta''$ ), and the loss tangent ( $\tan \alpha$ ) at the same frequencies. The agreement between transformed functions and those obtained directly from oscillatory measurements at frequencies ranging from  $7.91 \times 10^{-4}$  to  $1.5 \times 10^{-1}$  Hz. was generally good. Discrepancies at the extremities of this range were a result of the practical difficulties involved when creep measurements are made at very short times (representing high frequencies) and evaporation of water from the parallel plates of the rheogoniometer during low frequency dynamic experiments. Neither small strain technique alone covered the entire frequency or time range necessary for an

exhaustive study of semisolids. Creep data were unavoidably inaccurate at high frequencies, and the limitations of the rheogoniometer gear box prevented oscillatory measurements from being made at extremely low frequencies. The unification of data from oscillatory and creep measurements so as to provide a dynamic description over an extended frequency range ( $10^{-2}$ –25 Hz.) is discussed. The variations of each function with frequency are considered with reference to linear viscoelastic theory; the limiting values and the shapes of the plots at low frequencies agreed well with the theoretical values for viscoelastic liquids. It was concluded that such interconversion techniques are applicable and valuable for interpreting the rheological behavior of a pharmaceutical system.

**Keyphrases** □ Creams, oil-in-water, stabilized by mixed emulsifiers—viscoelastic properties, correlation between creep and oscillatory tests □ Creep measurements—correlation with oscillatory functions, oil-in-water creams stabilized by mixed emulsifiers □ Oscillatory functions—correlation with creep measurements, oil-in-water creams stabilized by mixed emulsifiers □ Viscoelastic properties, oil-in-water creams stabilized by mixed emulsifiers—correlation between creep and oscillatory tests

The rheological properties of semisolid preparations affect all stages of manufacture, and they should be considered in quality control. The release of medications from semisolid vehicles is sometimes related to these properties, so a knowledge of the rheological effects of changes in formulation may also be important for bioavailability studies.

In the past, a major difficulty encountered in the rheological evaluation of semisolid ointments and creams was how to obtain a true measure of consistency. The approach described frequently in the literature is to use a continuous shear technique and then to attempt to correlate derived parameters, e.g., spur points or yield values, with the qualitative terms "consistency

change" or "body." However, data from such experiments are often misleading and should be treated with caution. All continuous shear techniques measure the complex phenomenon of structure breakdown which, in turn, is a function of the test method. The material constants necessary to define viscoelastic (semisolid) materials, e.g., Newtonian viscosity and modulus of elasticity, are not derived.

To obtain true measures of consistency, it is necessary to employ fundamental experiments in which the semisolids are examined in their rheological ground states, i.e., when the method of testing does not significantly disrupt static structures. Small strain rheological experiments such as creep and oscillatory techniques are included in this category and have been used to investigate the rheological behavior of an extensive range of cosmetic and pharmaceutical materials (1-31). A suitable instrument for creep testing is the concentric cylinder reaction air turbine viscometer (22, 31-33). Oscillatory experiments may be performed using the Weissenberg rheogoniometer coupled to a Solartron digital transfer function analyzer and mechanical reference synchronizer (26).

For an exhaustive study of semisolids, it is usually necessary to employ both types of small strain experiment, because neither method alone determines viscoelastic properties over the required wide time or frequency range. Creep measurements essentially provide information at long times (equivalent to low frequencies that are inaccessible to the rheogoniometer) whereas the high frequency (short time) range is accessible only to dynamic experiments. Thus, a difficulty arises when attempts are made to compare the results of past studies, because a description of the mechanical behavior of the systems may be given by transient functions at long times such as compliances expressed as functions of time,  $J(t)$ , and by oscillatory functions at short times, such as storage and loss compliances expressed as functions of frequency,  $J'(\omega)$  and  $J''(\omega)$ .

However, fundamental parameters may be mathematically interconverted using linear viscoelastic theory. It is then possible to transform any one viscoelastic function derived in shear to any other, provided that the former is known over a sufficiently wide range of time or frequency. Thus, the comparison problem may be solved if functions are transformed so as to provide a unified parameter applicable at both high and low frequencies. Since the necessary exact calculations are often difficult and tedious, various approximation methods are usually employed (34-36). A comparatively simple numerical approximation for converting transient to dynamic data was described by Schwarzl (36).

The present investigation had two objectives:

1. To determine whether the conversion of creep data to dynamic functions is feasible for model pharmaceutical systems using Schwarzl's transformation formulas. If so, it may also be possible to derive dynamic data at very low frequencies, and oscillatory data may also be produced within the rheogoniometer's frequency range without using this expensive instrument.

2. To assess the accuracy involved in this method of transforming data in the light of the many variables

normally involved in creep and oscillatory experiments. These include the different viscometer geometries (parallel plate and concentric cylinder), the dissimilar times for which the emulsions remain in each viscometer before and during the experiments, that no allowance is made for end effects in creep or for evaporation effects (particularly from parallel plates) and the possibility that internal structure breaks down to different extents when the two viscometers are loaded.

Liquid paraffin-in-water emulsions containing cetostearyl alcohol and the surfactants cetrimide or cetomacrogol were chosen as model ionic and nonionic systems to represent pharmaceutical and cosmetic semisolids in general. These preparations have already been examined in detail by both fundamental methods, and information is available as to the effects of small changes in formulation on each type of viscoelastic function (13, 17, 20). To cover the consistency range usually found in pharmaceutical formulations, two emulsions were prepared from each mixed emulsifier, one a "soft" semisolid and the other a "stiff" material.

## EXPERIMENTAL

**Materials**—Cetostearyl alcohol, liquid paraffin, water, cetrimide<sup>1</sup>, and cetomacrogol<sup>2</sup> were as described previously (13, 17, 37).

**Preparation of Systems**—Liquid paraffin-in-water emulsions were made by a standardized procedure according to the formulas in Table I (13). Prior to testing, emulsions were stored for sufficient time at  $25 \pm 0.5^\circ$  to ensure that consistency build-up was complete and that the systems were not changing in rheological properties during the test. The microscopic and macroscopic appearances of each formulation were already described (1, 13, 14, 17, 18).

**Creep Tests**—Creep experiments were performed at  $25 \pm 0.5^\circ$  using a concentric cylinder reaction air turbine viscometer (22, 31, 33). Approximate linearity checks were made at short times, and the creep curves were recorded in the linear viscoelastic regions. Each creep stress was applied for a minimum of 90 min., by which time the strain or compliance responses for the samples were essentially linear with time. Creep curves were analyzed into discrete spectra using a method similar to that of Warburton and Barry (38). To check the accuracy of the analysis, a computer program was written to regenerate values of  $J(t)$  from the discrete spectral values. Agreement between experimental and reconstituted values for  $J(t)$  was better than 2% full-scale deflection, even at long times.

**Oscillatory Tests**—Oscillatory tests were performed at  $25 \pm 0.5^\circ$ . The instrument was employed with parallel plates, 7.5 cm. in diameter, and the platen gap was set to  $6.35 \times 10^{-2}$  cm. The torsion bar constant was  $2.207 \times 10^3$  dyne cm./ $2.54 \times 10^{-3}$  cm. movement. Initial tests for linearity were performed (20), and the systems were examined in their linear viscoelastic regions by applying sinusoidally varying shear strains at frequencies ranging from  $7.91 \times 10^{-4}$  to 25 Hz. ( $n$  Hz. =  $2\pi n$  rad./sec.). At each frequency, the amplitude ratio and the phase shift,  $\alpha$ , were determined and were employed to calculate the storage modulus ( $G'$ ) and the dynamic viscosity ( $\eta'$ ) using Walters' equations for parallel plate geometry (39, 40). The other viscoelastic functions,  $G''$ ,  $\eta''$ ,  $J'$ , and  $J''$ , were calculated from  $G'$  and  $\eta'$  using Eqs. 1-4 (34):

$$G'' = \eta' \omega \quad (\text{Eq. 1})$$

$$\eta'' = G' / \omega \quad (\text{Eq. 2})$$

$$J' = G' / (G'^2 + G''^2) \quad (\text{Eq. 3})$$

$$J'' = G'' / (G'^2 + G''^2) \quad (\text{Eq. 4})$$

<sup>1</sup> A commercial mixture of alkyl trimethylammonium bromides.

<sup>2</sup> A polyethylene glycol ether condensate of cetyl or cetostearyl alcohol with ethylene oxide; formula  $\text{CH}_2(\text{CH}_2)_{17}(\text{OCH}_2\text{CH}_2)_n\text{OH}$ .

<sup>3</sup> With a R14 Weissenberg rheogoniometer, modified to bring it up to R16 standards, coupled to a digital transfer function analyzer and mechanical reference synchronizer (20, 21, 26, 29, 30).

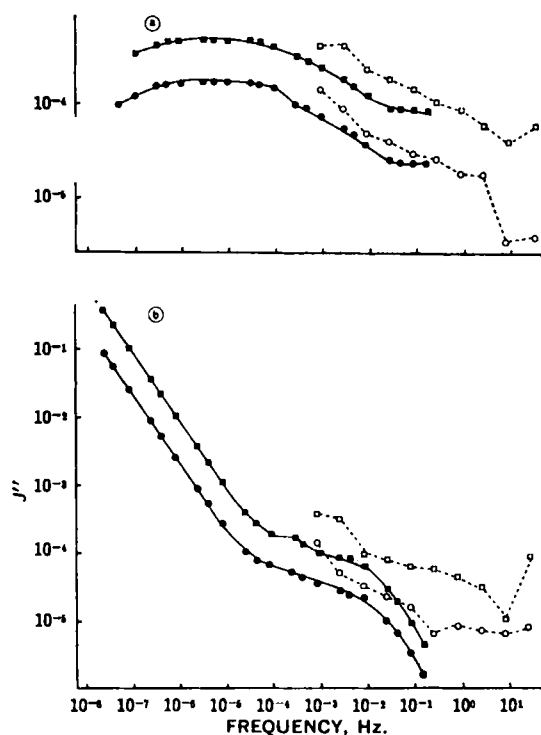


**Figure 1**—Cetrimide emulsions C8 and C14, showing the variation of: (a) storage compliance,  $J'$ , and (b) loss compliance,  $J''$  ( $\text{dyne}^{-1} \text{cm.}^2$ ), with frequency (Hz.). Key:  $\square$ , C8, and  $\circ$ , C14, values derived from oscillatory experiments using a rheogoniometer; and  $\blacksquare$ , C8, and  $\bullet$ , C14, theoretical values derived by transformation of creep data.

A description of these functions was given previously (20, 21). The storage modulus,  $G'$ , and the storage compliance,  $J'$ , are associated with energy stored and recovered per cycle of deformation; the loss modulus,  $G''$ , and the loss compliance,  $J''$ , are measures of energy lost or dissipated as heat during this time. The dynamic viscosity,  $\eta'$ , is another useful way of describing dissipative effects and is the real part of a complex viscosity. The imaginary part,  $\eta''$ , is related to stored energy. The loss tangent,  $\tan \alpha$ , is a useful parameter because, although it conveys no physical magnitude and is dimensionless, it is a measure of the ratio of energy lost to energy stored in a cyclic deformation.

**Numerical Calculation of Storage and Loss Compliances from Creep Compliance**—Schwarzl (36) published a number of formulas of increasing complexity but decreasing relative error with which to calculate the storage compliance,  $J'(\omega)$ , and the loss compliance,  $J''(\omega)$ , from the creep compliance,  $J(t)$ . Equations 5 and 6 are the most accurate for calculating  $J'$  and  $J''$ , respectively, if infinite series are to be avoided:

$$J'(\omega) \sim J(t) + 0.000715[J(32t) - J(16t)] - 0.0185[J(16t) - J(8t)] + 0.197[J(8t) - J(4t)] - 0.778[J(4t) - J(2t)] - 0.181[J(t) - J(t/2)] - 0.0494[J(t/4) - J(t/8)] \quad (\text{Eq. 5})$$

**Table I**—Composition of Emulsions (in Grams)

	C8 <sup>a</sup>	C14	N7	N16
Liquid paraffin	100	100	100	100
Water	300	300	300	300
Cetostearyl alcohol	28.8	50.4	25.2	57.6
Cetrimide	3.2	5.6	—	—
Cetomacrogol	—	—	2.8	6.4

<sup>a</sup> C represents cetrimide (cationic) emulsions, N represents cetomacrogol (nonionic) emulsions, and the associated numerals refer to the approximate percentage of mixed emulsifier (surfactant plus alcohol) present.

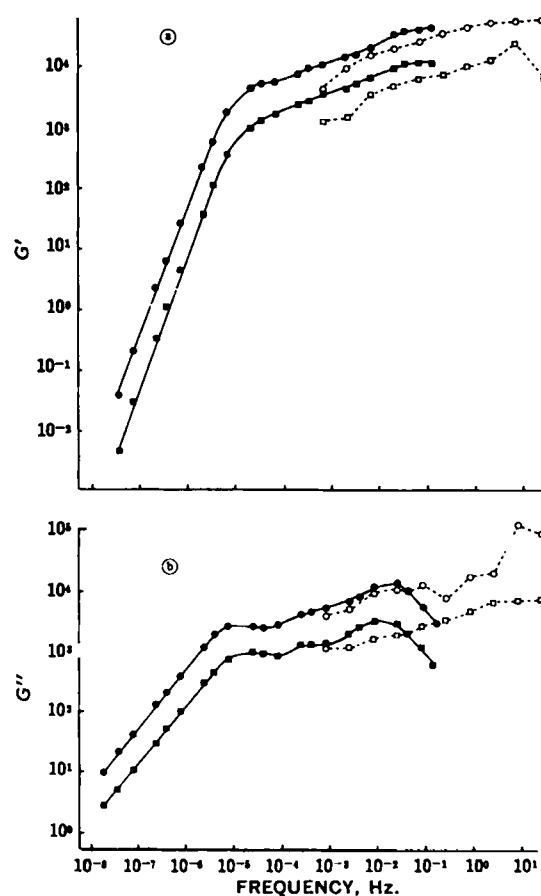


**Figure 2**—Cetrimide emulsions C8 and C14, showing the variation of: (a) storage modulus,  $G'$ , and (b) loss modulus,  $G''$  ( $\text{dynes cm.}^{-2}$ ), with frequency (Hz.). Key:  $\square$ , C8, and  $\circ$ , C14, values derived from oscillatory experiments using a rheogoniometer; and  $\blacksquare$ , C8, and  $\bullet$ , C14, theoretical values derived by transformation of creep data.

$$J''(\omega) \sim -0.470[J(4t) - J(2t)] + 1.674[J(2t) - J(t)] + 0.198[J(t) - J(t/2)] + 0.620[J(t/2) - J(t/4)] + 0.012[J(t/4) - J(t/8)] + 0.172[J(t/8) - J(t/16)] + 0.043[J(t/32) - J(t/64)] + 0.012[J(t/128) - J(t/256)] \quad (\text{Eq. 6})$$

where  $\omega$  ( $\text{rad. sec.}^{-1}$ ) =  $1/t$  sec.

The values of  $J(t)$  required for the calculations may be read directly from the experimental creep curve and inserted into Eqs. 5 and 6. However, as the curves had already been analyzed into discrete spectra, a computer program was written which converted discrete spectral results into the values of  $J(t)$  specified in the equations. It then processed the conversion of this data into  $J'(\omega)$  and  $J''(\omega)$ . Since the discrete analysis was available, these transformed data were checked and found to be accurate, using exact interrelationships (34).

The other oscillatory functions were calculated from the transformed values of  $J'$  and  $J''$  using Eqs. 2 and 7-9 (34):

$$G' = J'/(J'^2 + J''^2) \quad (\text{Eq. 7})$$

$$G'' = J''/(J'^2 + J''^2) \quad (\text{Eq. 8})$$

$$\tan \alpha = G''/G' \quad (\text{Eq. 9})$$

## RESULTS

The results of discrete spectral analyses of the creep curves are in Table II. Figures 1-4 show plots of the loss tangents and the storage and loss compliances, moduli, and viscosities versus frequency for cetrimide emulsions. The same functions for cetomacrogol emulsions are illustrated in Figs. 5-8. Each figure contains the appro-

**Table II—Discrete Spectral Analysis of Creep Curves [Three Voigt Unit, Residual Spring, and Residual Dashpot Model (38)]**

Viscoelastic Parameters*	Emulsions			
	C8	C14	N7	N16
Residual viscosity $\eta_0 (\times 10^6)$	19.2	79.1	4.38	40.8
Residual compliance $J_0 (\times 10^{-4})$	0.90	0.247	1.55	0.272
Viscosity $\eta_1 (\times 10^6)$	4.32	14.5	1.38	10.1
Compliance $J_1 (\times 10^{-4})$	2.20	0.823	6.82	1.20
Retardation time $\tau_1$	949	1190	943	1210
Viscosity $\eta_2 (\times 10^6)$	2.18	5.40	2.60	5.18
Compliance $J_2 (\times 10^{-4})$	0.691	0.300	1.29	0.849
Retardation time $\tau_2$	150	162	341	220
Viscosity $\eta_3 (\times 10^6)$	2.66	7.19	1.25	6.81
Compliance $J_3 (\times 10^{-4})$	1.06	0.318	1.64	0.441
Retardation time $\tau_3$	28.0	23.0	20.0	30.0

\* Viscosities, compliances, and retardation times are in units of poise,  $\text{dyne}^{-1} \text{cm}^2$ , and sec., respectively.

appropriate function derived by direct oscillatory measurements at frequencies ranging from  $10^{-4}$  to 25 Hz. and the same function calculated from the creep data in Table II using Eqs. 5-9. Transformed data are plotted over the frequency range  $10^{-2}$ - $1.5 \times 10^{-1}$  Hz.

### DISCUSSION

In general, agreement between experimental storage and loss parameters obtained using the rheogoniometer and the same functions calculated from creep data using Schwarzl's (36) transformations is good (Figs. 1-8). The significance of this is apparent when considering both the nature of the mathematical approximations

and the many variables involved in the experiments (see introductory material). This agreement between the data provides strong evidence that the basic assumption made in previous work is valid; that is, that neither small strain technique destroys static structure and thus the systems are examined essentially in their rheological ground states during both types of measurement.

Creep data imply that the emulsions were of a slightly higher consistency during transient experiments than when observed in oscillation. Thus, in Figs. 1-8 a slight trend is apparent whereby transformed compliances are lower and transformed viscosities and moduli are higher than the corresponding parameters derived directly from oscillatory experiments. The most likely explanation of this trend involves two factors.

1. The loading process in the rheogoniometer destroys slightly more structure because of the relatively high shear rates and shear strains applied when parallel plates are brought together.
2. Neglect of the "end effect" in creep calculations increases the value used for the mean shear stress. If the end effect were allowed for, the rheological parameters would move closer to the relevant oscillatory data.

At high frequencies, data were transformed from values of  $J(t)$  taken within a few seconds of creep. It is not possible to measure accurately these compliances because of the inertias of the viscometer and recorder. Thus, in this region, data for transformed functions are often scattered and tend to deviate from the experimental points. At the other end of the frequency range, oscillatory measurements involve errors, mainly because of evaporation from the parallel plates during the comparatively long experimental time (20, 21). Sometimes these points are also scattered. However, these discrepancies are slight and the accuracy of the transformation is excellent in view of the many experimental variables and the mathematical approximations made.

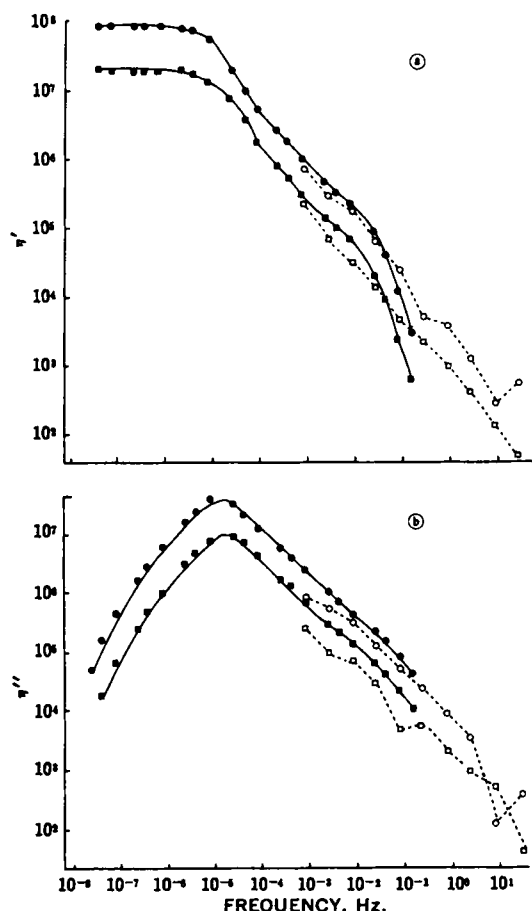


**Figure 3—Cetrimide emulsions C8 and C14, showing the variation of: (a) dynamic viscosity,  $\eta'$ , and (b) imaginary part of a complex viscosity,  $\eta''$  (poises), with frequency (Hz.). Key:  $\square$ , C8, and  $\circ$ , C14, values derived from oscillatory experiments using a rheogoniometer; and  $\blacksquare$ , C8, and  $\bullet$ , C14, theoretical values derived by transformation of creep data.**

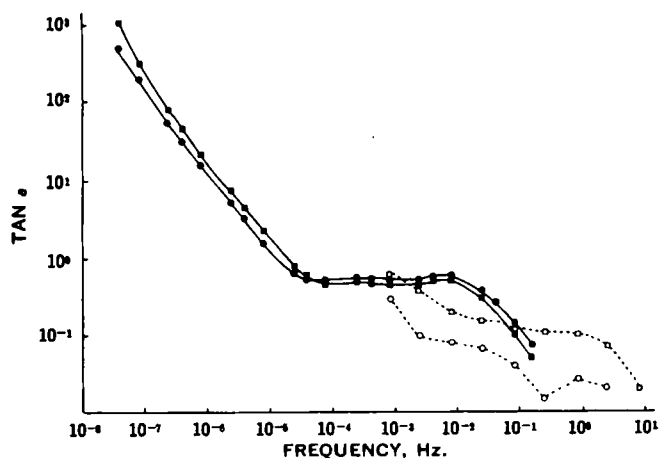


**Figure 4—Cetrimide emulsions C8 and C14, showing the variation of loss tangent,  $\tan \delta$ , with frequency (Hz.). Key:  $\square$ , C8, and  $\circ$ , C14, values derived from oscillatory experiments using a rheogoniometer; and  $\blacksquare$ , C8, and  $\bullet$ , C14, theoretical values derived by transformation of creep data.**

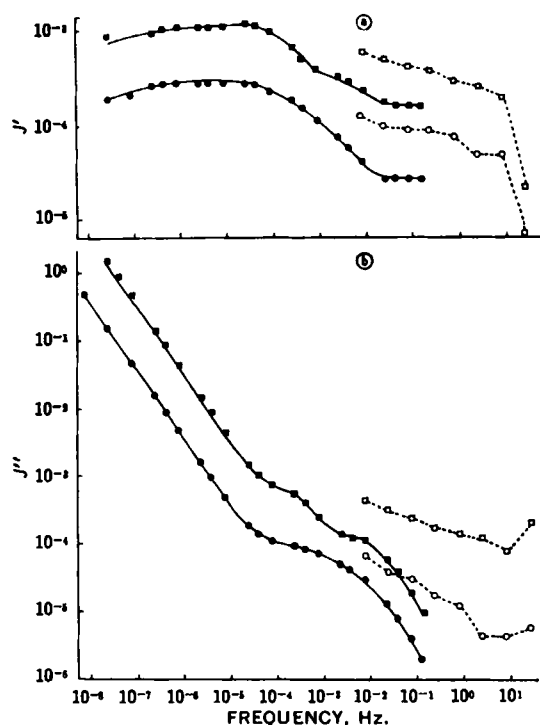


**Figure 5**—Cetomacrogol emulsions N7 and N16, showing the variation of: (a) storage compliance,  $J'$ , and (b) loss compliance,  $J''$  ( $\text{dyne}^{-1} \text{cm.}^2$ ), with frequency (Hz.). Key:  $\square$ , N7, and  $\circ$ , N16, values derived from oscillatory experiments using a rheogoniometer; and  $\blacksquare$ , N7, and  $\bullet$ , N16, theoretical values derived by transformation of creep data.

Since the transformed dynamic functions were similar to those obtained from direct dynamic measurements over the frequency range  $7.91 \times 10^{-4}$  (cetrimide) or  $7.91 \times 10^{-3}$  (cetomacrogol) to  $1.5 \times 10^{-1}$  Hz., it was deduced that transformed data extrapolated to low frequencies are also representative of the values that would be obtained if it were possible to conduct oscillatory experiments in this frequency range. In practice, one cannot perform reliable oscillatory experiments at frequencies below approximately  $10^{-4}$  Hz. because of the limitations of the rheogoniometer and the transfer function analyzer and because of evaporation effects from parallel plates.

Thus, it is concluded that the described transformation procedure provides reasonably accurate dynamic functions at intermediate frequencies so that it is possible to obtain dynamic data without an oscillatory instrument. This procedure also enables oscillatory functions to be calculated at frequencies lower than those accessible to an oscillatory instrument.

Now that it has been established that transformation procedures are applicable to pharmaceutical materials and an understanding has been reached of the limitations of both creep and oscillatory experiments with regard to frequency range, it is possible to suggest a practical procedure for examining the viscoelastic properties of such formulations. In this process, data are selected from both types of experiment in the time-frequency range where each method is most accurate. This involves using high frequency values obtained from direct oscillatory measurements and low frequency values realized when creep data are transformed. Typical examples are shown in Fig. 9, where data taken from Figs. 2 and 3 are collated to provide single plots of the variations of  $G'$  and  $\eta'$  with frequency. To obtain smooth plots, less emphasis is given to high frequency transformed functions and to low frequency oscillatory values. The functions in the other graphs (Figs. 1–8) can be similarly processed to obtain smooth plots (not shown here). The advantage of this unification procedure is that one now obtains a clear rheological description over the entire frequency range by means of a single type of response function.

Although a viscoelastic material may be rheologically defined by any one of the viscoelastic functions used in this work, it is considered valuable to examine several functions because different

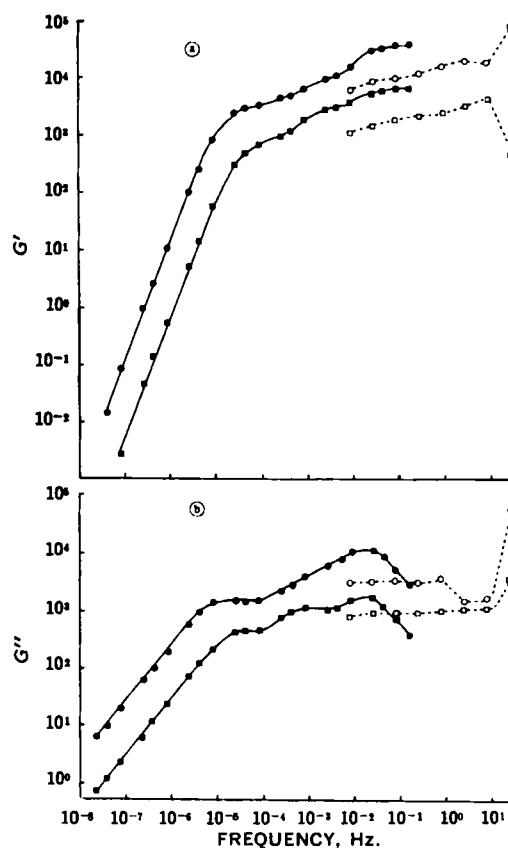


**Figure 6**—Cetomacrogol emulsions N7 and N16, showing the variation of: (a) storage modulus,  $G'$ , and (b) loss modulus,  $G''$  ( $\text{dynes cm.}^{-2}$ ), with frequency (Hz.). Key:  $\square$ , N7, and  $\circ$ , N16, values derived from oscillatory experiments using a rheogoniometer; and  $\blacksquare$ , N7, and  $\bullet$ , N16, theoretical values derived by transformation of creep data.

types of viscoelastic behavior often exhibit different degrees of prominence in the various plots. For both ionic and nonionic preparations, as the mixed emulsifier concentration increased, consistencies rose as coherent viscoelastic networks formed in the continuous phases (1).

This is shown throughout the entire frequency range by increases in the experimental and transformed viscosities and moduli and decreases in the compliances as the cetrimide and cetomacrogol mixed emulsifier concentrations rise from 8 to 14 and 7 to 16%, respectively. The loss tangent decreases with concentration, indicating that, when networks build up, the elastic component increases to a greater extent than the viscous component. The trends exhibited by the functions plotted in Figs. 1–9 are similar to those shown by uncrosslinked viscoelastic polymers (34) and conform with a generalized Maxwell model analogy described previously (20). At high frequencies, elastic behavior dominates because there is little time available for viscous deformation, and values of  $G'$  and  $J'$  are high and low, respectively. As the time period increases, viscous behavior becomes increasingly prominent, and  $J'$  rises and  $G'$  falls with decrease in frequency. Plots of both functions alter generally in the  $8 \times 10^{-5}$ – $1 \times 10^{-4}$ -Hz. frequency region (Figs. 1, 2, 5, 6, 9).

Although  $\eta''$  is not usually used to describe viscoelastic deformation, plots are included here to complete the data (Figs. 3b and 7b). These also change, exhibiting pronounced maxima in this region. These variations are significant, because they occur at frequencies that correspond to creep times ( $\sim 1600$ – $2000$  sec.) only slightly greater than the longest retardation times obtained by the discrete spectral analyses of the curves (*cf.*, Table II). They indicate that retarded elastic effects no longer operate and further deformation at low frequencies is due to viscous flow. Thus, at very low frequencies (much less than  $10^{-8}$  Hz.),  $G'$  and  $\eta''$  fall rapidly and  $J'$  flattens, as the energy stored per cycle becomes negligible compared to that dissipated. Viscoelastic theory predicts that, at these low frequencies,  $G'$  plots should approach zero with a slope of 2 and  $J'$

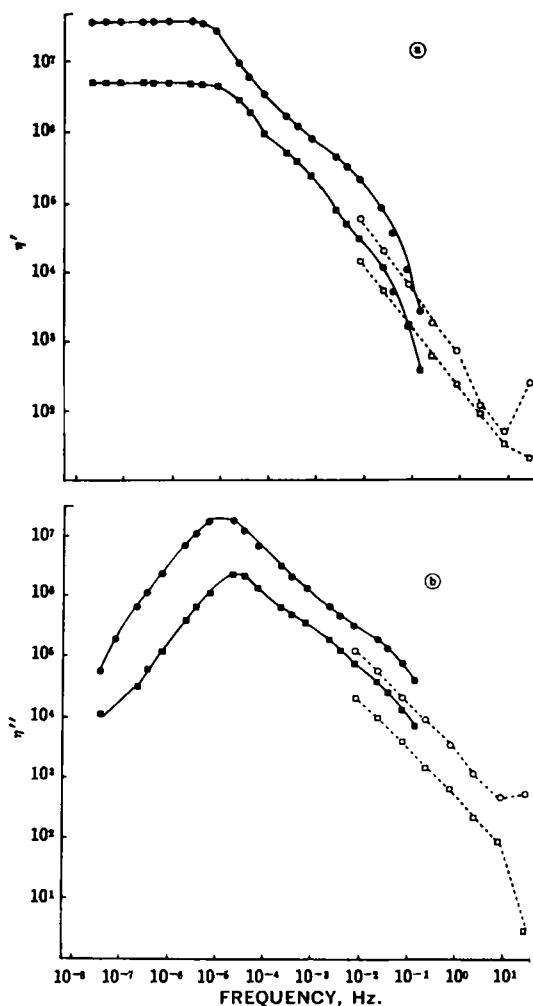


**Figure 7**—Cetomacrogol emulsions N7 and N16, showing the variation of: (a) dynamic viscosity,  $\eta'$ , and (b) imaginary part of a complex viscosity,  $\eta''$  (poises), with frequency (Hz.). Key:  $\square$ , N7, and  $\circ$ , N16, values derived from oscillatory experiments using a rheogoniometer; and  $\blacksquare$ , N7, and  $\bullet$ , N16, theoretical values derived by transformation of creep data.

plots should approach  $J_e$ , the total recoverable (elastic) compliance in creep. The results summarized in Table III show that agreement between such theoretical and transformed data is good. At high frequencies,  $G'$  values should approach  $G_0$ , the instantaneous elastic modulus derived in creep. The values in Table II indicate that this condition is met quite closely. Such agreement is especially satisfactory in the light of the experimental limitations involved in short time creep testing, *i.e.*, the inertial effects of the viscometer and the difficulty in applying a truly instantaneous stress.

Plots of the dissipative functions  $\eta'$ ,  $G''$ , and  $J''$  also inflect at frequencies close to  $10^{-5}$ – $10^{-4}$  Hz.; at lower frequencies, dissipative mechanisms predominate and  $G''$  reduces,  $J''$  increases, and  $\eta'$  flattens out. In regions where  $G'$  changes relatively slowly with frequency (greater than approximately  $10^{-4}$  Hz.), the behavior is predominately elastic and  $G''$  is slightly less and  $J''$  is slightly greater than the corresponding storage parameters. In addition, when  $\eta'$  flattens,  $G''$  rises steeply, and when  $\eta'$  increases rapidly,  $G''$  shows little variation. At the very low frequencies that correspond to long creep times,  $\eta'$  approaches the creep residual viscosity,  $\eta_0$ , and  $J''$  and  $G''$  slopes are close to  $-1$  and  $+1$ , respectively, as predicted by viscoelastic theory (Table III).

Plots of the variation of  $\tan \alpha$  with frequency (Figs. 4 and 8) are of considerable practical interest because each emulsion has a characteristic curve containing maxima and minima. Loss tangent plots have been referred to as "consistency spectra" because of their similarities with the spectra obtained from spectrophotometry (29). At very low frequencies (less than  $10^{-5}$  Hz.),  $\tan \alpha$  is large and, as

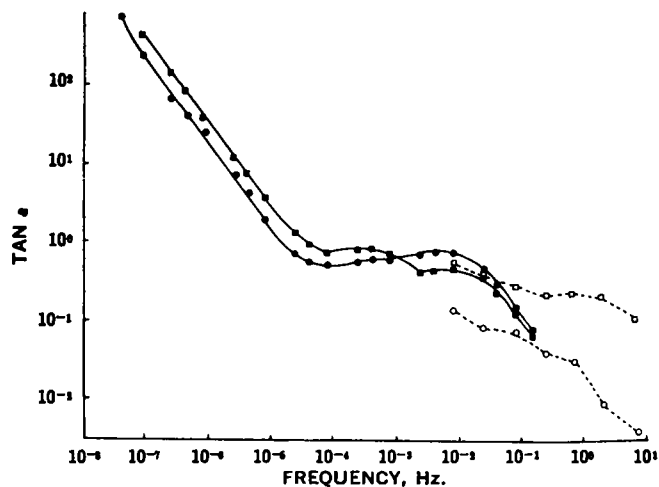


**Figure 8**—Cetomacrogol emulsions N7 and N16, showing the variation of loss tangent,  $\tan \alpha$ , with frequency (Hz.). Key:  $\square$ , N7, and  $\circ$ , N16, values derived from oscillatory experiments using a rheogoniometer; and  $\blacksquare$ , N7, and  $\bullet$ , N16, theoretical values derived by transformation of creep data.

predicted by theory, it is inversely proportional to the frequency so the plots in this region have slopes of  $-1$  (Table III). In the frequency region where all other plots change ( $\sim 10^{-4}$  Hz.), spectra flatten with  $\tan \alpha$  values close to unity. In the intermediate and high frequency regions, all spectra contain at least three minima which are possibly related to retardation mechanisms.

## CONCLUSIONS

1. Liquid paraffin-in-water emulsions stabilized by mixed emulsifiers of the cetrimide or cetomacrogol surfactants—cetostearyl alcohol type were used as model systems to represent pharmaceutical semisolids. They were examined in their linear viscoelastic regions using creep (concentric cylinder reaction air turbine viscometer) and oscillatory (parallel plate Weissenberg rheogoniometer) techniques.

2. Storage and loss compliances ( $J'$  and  $J''$ ) for frequencies ranging from  $2.5 \times 10^{-8}$  to  $1.5 \times 10^{-1}$  Hz. were calculated from creep data using numerical formulas (29). These were used to de-

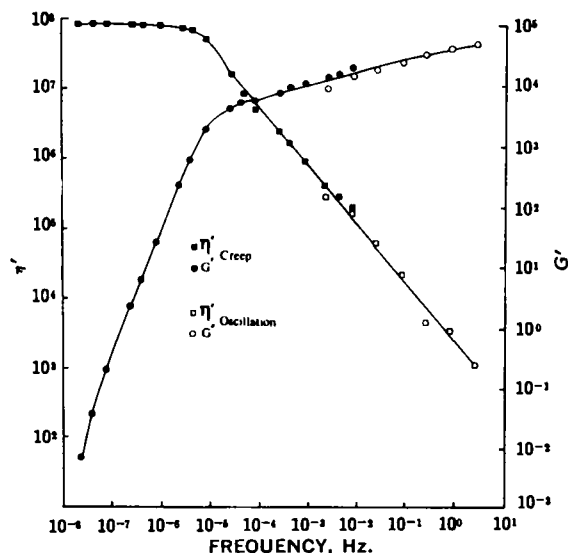


**Figure 9**—Cetrimide emulsion C8. Unified plots of the variations of storage modulus,  $G'$  (dynes  $\text{cm}^{-2}$ ), and dynamic viscosity,  $\eta'$  (poises), with frequency (Hz.). Low frequency values were derived by transformation of creep data, and high frequency values were derived from oscillatory experiments using a rheogoniometer.

**Table III—Relationships between Viscoelastic Data**

Data	Emulsions			
	C8	C14	N7	N16
Slope of $G'$ plots at low frequencies (theoretical value = 2 dynes cm. <sup>-2</sup> Hz. <sup>-1</sup> )	2.1	2.1	2.1	2.1
Slope of $G''$ plots at low frequencies (theoretical value = 1 dyne cm. <sup>-2</sup> Hz. <sup>-1</sup> )	1.0	1.0	1.0	1.0
Comparison of slope of $J'$ plots at low frequencies and (in parentheses) $J_s$ derived in creep (dyne <sup>-1</sup> cm. <sup>3</sup> )	$5.0 \times 10^{-4}$ ( $4.3 \times 10^{-4}$ )	$1.5 \times 10^{-4}$ ( $1.7 \times 10^{-4}$ )	$1.0 \times 10^{-3}$ ( $1.1 \times 10^{-3}$ )	$3.0 \times 10^{-4}$ ( $2.4 \times 10^{-4}$ )
Comparison of $\eta'$ derived at low frequencies and (in parentheses) $\eta_0$ derived in creep (poises)	$2.0 \times 10^7$ ( $2.0 \times 10^7$ )	$7.9 \times 10^7$ ( $7.9 \times 10^7$ )	$4.8 \times 10^8$ ( $4.4 \times 10^8$ )	$3.8 \times 10^7$ ( $4.1 \times 10^7$ )
Slope of consistency spectra plots at low frequencies (theoretical value = -1 Hz. <sup>-1</sup> )	-1.1	-1.1	-1.0	-1.1
Comparison of residual shear modulus $G_0$ derived in creep and (in parentheses) $G'$ at 7.91 and 25 Hz., respectively ( $\times 10^4$ dynes cm. <sup>-2</sup> )	1.1 (2.3, 0.6)	4.0 (4.9, 5.0)	0.65 (0.45, 0.05 <sup>a</sup> )	3.7 (1.9, 7.5)

<sup>a</sup> Low value due to nonlinear response at 25 Hz.

termine the other dynamic functions,  $G'$ ,  $G''$ ,  $\eta'$ ,  $\eta''$ , and  $\tan \alpha$ , at the same frequencies.

3. The transformed dynamic functions were compared with the same functions obtained directly from oscillatory measurements at frequencies ranging from  $7.91 \times 10^{-4}$  to  $1.5 \times 10^{-1}$  Hz. for cetrimide emulsions and from  $7.91 \times 10^{-3}$  to  $1.5 \times 10^{-1}$  Hz. for cetomacrogol emulsions. Agreement was excellent at most frequencies; discrepancies at the extremes of the range were because of unavoidable experimental variables. This good agreement suggests that dynamic descriptions of pharmaceutical semisolids may be obtained at intermediate frequencies using a creep viscometer when an expensive rheogoniometer with associated transfer function analyzer is not available.

4. Neither small strain technique alone covered the entire time scale necessary for an exhaustive study of pharmaceutical semisolids. Creep data were unavoidably inaccurate at high frequencies, and oscillatory measurements could not be made at very low frequencies. To solve this problem, it was shown that creep and oscillatory data may be collated and unified so as to provide smooth plots of the variation of each dynamic function over an extended frequency range ( $10^{-3}$ -25 Hz.). This unification procedure uses high frequency values obtained from oscillatory measurements and low frequency values transformed from creep experiments.

5. The variations of each dynamic function with frequency over the entire frequency range were discussed with reference to linear viscoelastic theory. The limiting values and the shapes of the plots agreed well with the theoretical values for viscoelastic liquids.

**NOMENCLATURE**

- C = cetrimide (cationic) emulsions
- $G'$  = storage shear modulus
- $G''$  = loss shear modulus
- $G_0$  = residual shear modulus (creep)
- $J$  = creep shear compliance
- $J'$  = storage shear compliance
- $J''$  = loss shear compliance
- $J_s$  = total elastic shear compliance (creep)
- $J_0$  = residual shear compliance (creep)

- $J_1, J_2, J_3$  = shear compliances of Voigt units 1, 2, and 3, respectively (creep)
- N = cetomacrogol (nonionic) emulsion
- $\alpha$  = phase angle
- $n$  = frequency of oscillation (hertz)
- $t$  = time (second)
- $\eta'$  = real component of complex dynamic viscosity; dynamic viscosity
- $\eta''$  = imaginary component of complex dynamic viscosity
- $\eta_0$  = residual shear viscosity (creep)
- $\eta_1, \eta_2, \eta_3$  = shear viscosities of Voigt units 1, 2, and 3, respectively (creep)
- $\tau_1, \tau_2, \tau_3$  = retardations times of Voigt units 1, 2, and 3, respectively (creep)
- $\omega$  = frequency of oscillation (rad. sec.<sup>-1</sup>)

**REFERENCES**

- (1) B. W. Barry and G. M. Eccleston, *J. Texture Studies*, **3**, 324 (1972).
- (2) B. W. Barry, *ibid.*, **1**, 405(1970).
- (3) B. W. Barry, *J. Soc. Cosmet. Chem.*, **22**, 487(1971).
- (4) S. S. Davis, *Amer. Perfum. Cosmet.*, **85**, 45(1970).
- (5) B. W. Barry and B. Warburton, *J. Soc. Cosmet. Chem.*, **19**, 725(1968).
- (6) B. W. Barry, *Mfg. Chem. Aerosol News*, Apr. 1971, 27.
- (7) B. W. Barry, *Rheol. Acta*, **10**, 96(1971).
- (8) B. W. Barry and A. J. Grace, *J. Texture Studies*, **2**, 259 (1971).
- (9) B. W. Barry and E. Shotton, *J. Pharm. Pharmacol., Suppl.*, **19**, 121S(1967).
- (10) B. W. Barry, *J. Colloid Interface Sci.*, **28**, 82(1968).
- (11) *Ibid.*, **32**, 551(1970).
- (12) B. W. Barry, *J. Pharm. Pharmacol.*, **25**, 131(1973).
- (13) B. W. Barry and G. M. Saunders, *J. Colloid Interface Sci.*, **34**, 300(1970).
- (14) B. W. Barry and G. M. Saunders, *J. Pharm. Pharmacol., Suppl.*, **22**, 139S(1970).

- (15) B. W. Barry and G. M. Saunders, *J. Colloid Interface Sci.*, **35**, 689(1971).  
 (16) *Ibid.*, **36**, 130(1971).  
 (17) *Ibid.*, **38**, 616(1972).  
 (18) *Ibid.*, **38**, 626(1972).  
 (19) *Ibid.*, **41**, 331(1972).  
 (20) B. W. Barry and G. M. Eccleston, *J. Pharm. Pharmacol.*, **25**, 244(1973).  
 (21) *Ibid.*, **25**, 394(1973).  
 (22) B. W. Barry and A. J. Grace, *J. Pharm. Pharmacol.*, **22**, 147S(1970).  
 (23) B. W. Barry and A. J. Grace, *Rheol. Acta*, **10**, 113(1971).  
 (24) B. W. Barry and A. J. Grace, *J. Pharm. Sci.*, **60**, 814(1971).  
 (25) *Ibid.*, **60**, 1198(1971).  
 (26) B. Warburton and S. S. Davis, *Rheol. Acta*, **8**, 205(1969).  
 (27) S. S. Davis, *J. Pharm. Sci.*, **58**, 412(1969).  
 (28) *Ibid.*, **58**, 418(1969).  
 (29) *Ibid.*, **60**, 1351(1971).  
 (30) *Ibid.*, **60**, 1356(1971).  
 (31) G. M. Saunders, Ph.D. thesis, Portsmouth Polytechnic, Portsmouth, U. K., 1971.  
 (32) S. S. Davis, J. J. Deer, and B. Warburton, *J. Sci. Instr., Series 2*, **1**, 933(1968).  
 (33) B. W. Barry and G. M. Saunders, *J. Pharm. Pharmacol.*, **21**, 607(1969).  
 (34) J. D. Ferry, "Viscoelastic Properties of Polymers," Wiley, New York, N. Y., 1970, pp. 59-108.  
 (35) L. C. E. Struik and F. R. Schwarzl, *Rheol. Acta*, **8**, 134 (1969).  
 (36) F. R. Schwarzl, *ibid.*, **8**, 6(1969).  
 (37) B. W. Barry and G. M. Saunders, *J. Pharm. Sci.*, **60**, 645 (1971).  
 (38) B. Warburton and B. W. Barry, *J. Pharm. Pharmacol.*, **20**, 255(1968).  
 (39) K. Walters, "Basic Concepts and Formulae for the Rheogoniometer," Sangamo Controls, Bognor, England, 1968, pp. 15, 16.  
 (40) K. Walters and R. A. Kemp, *Rheol. Acta*, **7**, 1(1968).

#### ACKNOWLEDGMENTS AND ADDRESSES

Received May 9, 1973, from the *School of Pharmacy, Portsmouth Polytechnic, King Henry I Street, Portsmouth, United Kingdom.*

Accepted for publication August 1, 1973.

The authors thank the School of Pharmacy, University of London, for the use of the Weissenberg rheogoniometer.

\* Present address: Pharmaceutics Research Group, Department of Pharmacy, University of Aston in Birmingham, Gosta Green, Birmingham, 4, United Kingdom.

▲ To whom inquiries should be directed.

## Effect of Sodium Taurodeoxycholate on Biological Membranes: Release of Phosphorus, Phospholipid, and Protein from Everted Rat Small Intestine

STUART FELDMAN<sup>▲</sup>, MARK REINHARD, and CHARLES WILLSON

**Abstract** □ Sodium taurodeoxycholate accelerates the release of total phosphorus, lipid phosphorus, and protein from isolated everted rat small intestinal sacs. The effect occurs at concentrations of the physiological surfactant above the CMC. The effect of sodium taurodeoxycholate on components of the biological membrane can be related to an increase in permeability of the everted intestine to phenol red in the presence of various concentrations of the surfactant. The interaction of the surfactant with the biological membrane may produce an acceleration of the loss of structural integrity of the preparation, resulting in an increased permeability to phenol red.

**Keyphrases** □ Sodium taurodeoxycholate—effect on biological membranes, release of phosphorus, phospholipid, and protein from the everted rat small intestine, loss of structural integrity proposed □ Membranes, biological, everted rat small intestine—effect of sodium taurodeoxycholate on release of phosphorus, phospholipid, and protein □ Surfactants—effect of sodium taurodeoxycholate on release of phosphorus, phospholipid, and protein from the everted rat small intestine □ Permeability, everted rat small intestine—effect of sodium taurodeoxycholate on transport of phenol red, release of phosphorus, phospholipid, and protein from membrane, loss of structural integrity proposed

Previous investigators (1-7) showed an increase in drug absorption across biological membranes in the presence of physiological surfactants. An increase was found in the rate of transfer of salicylate (1) and salicylamide (2) across the everted rat small intestine in the

presence of micellar sodium taurodeoxycholate. Absorption of orally administered riboflavin in man increased upon coadministration of sodium deoxycholate, an unconjugated bile salt (3). The GI absorption of phenol red in the rat increased when phenol red was administered with sodium deoxycholate (4). Increased absorption of a number of drugs in the presence of bile salts was reported (5, 6) using an *in situ* perfusion technique. The influence of sodium taurodeoxycholate on the pharmacological effect (time required to produce overturn) of pentobarbital and ethanol in goldfish was studied (7). All these effects are presumably due to an alteration in the permeability of the biological membrane to these drugs by the physiological surfactant.

The exact mechanism of action of the physiological surfactants in increasing the permeability of biological membranes has not been elucidated, although it was postulated (1, 2, 4) that the mechanism may involve changes in membrane structure, possibly by solubilizing lipid components of the membrane. Bile salts were shown to solubilize phospholipids (8), a major component of biological membranes (9).

In a later study (10), the addition of lecithin, a phospholipid, or a mixture of fatty acids and esters to the micellar bile salt solution resulted in a reduction of the permeability effect of the bile salt on the everted rat intestine to salicylate ion. It was, therefore, decided to